Energy Reports 12 (2024) 2933–2945

Contents lists available at ScienceDirect

Energy Reports

journal homepage: www.elsevier.com/locate/egyr

Optimizing energy-efficient building renovation: Integrating double-skin façades with solar systems in the Mediterranean landscape

G. Barone [a], I. Vardopoulos [b], S. Attia [c], C. Vassilliades [d,e,*]

[a] Department of Industrial Engineering - University of Naples Federico II, P.le Tecchio, 80, Naples 80125, Italy
[b] School of Environment, Geography and Applied Economics, Harokopio University of Athens (HUA), Kallithea, Attica EL-17676, Greece
[c] Sustainable Building Design Lab, Dept. UEE, Faculty of Applied Sciences, University of Liège, Liège 4000, Belgium
[d] School of Architecture, Land and Environmental Sciences, Neapolis University Pafos (NUP), Pafos 8042, Cyprus
[e] Architecture Group, Department of Civil, Environmental and Natural resources engineering, Luleå University of Technology, Luleå 97187, Sweden

ARTICLE INFO

Keywords:
Retrofitting
Energy Performance
Building Envelope
Parametric Analysis
Sustainable Architecture

ABSTRACT

According to the European Environment Agency, 85–95 % of today's buildings will still be standing in 2050. As a result, there is an urgent need to renovate existing buildings to reduce energy consumption and improve their energy performance. The use of double-skin façades (DSFs) integrated with active solar systems is a promising solution for energy-efficient retrofitting of buildings in Europe. A DSF with integrated PVs is a building envelope system consisting of two layers of materials separated by an air gap, with the outer layer incorporating solar panels to harness solar energy for electricity generation while providing additional thermal insulation and environmental control benefits. This paper explores the use of DSF with integrated solar active systems in Mediterranean countries, aiming to find the optimal solution for the energy-efficient renovation of the building stock. A parametric analysis is carried out, and the results show that the use of DSFs in multi-story existing buildings can be sustainable, as it saves energy without the need of adding insulation in the building. Specifically, results indicate that selecting a DSF with a depth of less than 7.0 m yields a reduction in heating demands ranging from −5.49 % to −0.82 %. Conversely, when contemplating cooling loads, a substantial DSF configuration exceeding 6.0 m in depth is the preferred option, facilitating a reduction in cooling loads. Additionally, the depth of the air gap cavity significantly influences electricity production, with increased depth leading to enhanced electrical efficiency and higher electricity production, *i.e.* from approximately 18.6 kW for the smallest cavity depth to a peak of around 26.8 kW for the greatest depth. The findings of this study can contribute to the development of effective policies and strategies for sustainable building renovation in Mediterranean countries.

1. Introduction

The global climate crisis has reached a critical stage since its emergence in the early 1970s with the first oil crisis (Tombazis, 1994), and urgent actions are needed to mitigate its effects (Buonomano et al., 2022). This is making the building industry develop a concentrated effort to reduce building energy needs since they are responsible for a significant portion of the energy consumption and greenhouse gas emissions (Vassiliades et al., 2023), which makes the building sector a crucial area for implementing energy-saving solutions (Vardopoulos et al., 2023a) —the European building sector accounts for 24 % of the greenhouse gas emissions when the building sector in the world accounts for over 40 % of the total primary energy consumption (Anon, 2009).

On the other hand, the aging building stock in Europe (Vardopoulos et al., 2023b) poses a significant challenge to the reduction of energy consumption and greenhouse gas emissions (Savvides and Vassiliades, 2017). The European Union has set ambitious targets to promote energy renovation of buildings to reduce their carbon footprint and increase energy efficiency (Karytsas et al., 2019). Specifically, the European Union has set a target to reduce greenhouse gas emissions by 40 % below the 1990 level by 2030 (Vardopoulos, 2018). To achieve this, the EU has launched several initiatives and policies, including the Energy Performance of Buildings Directive (EPBD) (Energy Performance of Buildings Directive, 2018), which aims to improve the energy efficiency of buildings by promoting energy-efficient renovations (Vardopoulos et al., 2024a). The EPBD requires all EU member states to establish long-term renovation strategies that ensure a decarbonized building stock by 2050 (Rosenow et al., 2017). The EU also has a goal of achieving a nearly

* Corresponding author at: School of Architecture, Land and Environmental Sciences, Neapolis University Pafos (NUP), Pafos 8042, Cyprus.
E-mail address: c.vassiliades@nup.ac.cy (C. Vassilliades).

https://doi.org/10.1016/j.egyr.2024.08.032
Received 20 February 2024; Received in revised form 15 July 2024; Accepted 12 August 2024

Nomenclatures

Acronyms

PCM	phase change materials
BIPV	building integrated photovoltaic
BIPVT	building integrated photovoltaic thermal
PV	photovoltaic
DSF	double-skin façade
DF	double façade
SHGC	solar heat gain coefficient
COP	coefficient of performance
EPBD	Energy Performance of Buildings Directive
HVAC	Heating, ventilation, and air conditioning
i.e.	Latin; id est, meaning "in other words", "that is"
et al.	Latin; et al.ia (neuter), meaning "and others"
e.g.	Latin; exempli gratia, meaning "for example"

Symbols

m	meter
m^2	square meter
m^3	cubic metre
V	volume [m^3]
T	temperature [°C]
D	depth [m]
dy	infinitesimal height [m]
h	convective heat transfer coefficient [W/(m^2K)]
U	Thermal transmittance [W/(m^2K)]
CO_2	Carbon dioxide chemical formula
c	specific heat [kJ/(kg•K)]
W	watt
J	joule
kg	kilogram

Subscripts

air	air
c	convective
g	glass
a	air
w	wall
PV	photovoltaic panel

Greek

ρ	density [kg/m^3]

zero-energy building (nZEB) standard for all new buildings by the end of 2020 and for all buildings, including existing ones, by 2050 (Aste et al., 2017).

1.1. State of the art

To achieve the goals set, a number of measures and solutions need to be applied to the existing building stock across several climatic conditions, from the north to the south (Barone et al., 2023a). There are numerous methods for energy renovation of buildings, ranging from simple measures like insulation, high-performance windows, and energy-efficient HVAC and lighting (Italos et al., 2022; Theokli et al., 2021; Michael et al., 2020; Asdrubali et al., 2022) to more advanced technologies like the building integration of renewable energy systems and the implementation of double skin façades (Athienitis et al., 2018). Among these methods, the use of DSFs and building integrated active solar energy systems has gained significant attention in recent years due to their potential to reduce energy consumption and promote renewable energy use (Ioannidis et al., 2017, 2020).

A DSF is a building envelope system that consists of two layers of glass or other transparent materials separated by an air gap (Vassiliades et al., 2022a). Building integrated active solar energy systems, on the other hand, refer to systems that integrate solar collectors or PV panels into the building envelope or structure (Probst and Roecker, 2011; Vassiliades et al., 2019). These renewable-based systems can generate renewable energy on-site and contribute to the energy needs of the building (Savvides et al., 2024). The combination of DSFs and building-integrated active solar energy systems can provide significant benefits for energy renovation of buildings, such as reducing energy consumption for heating and cooling (Theokli et al., 2021), improving indoor air quality (Barone et al., 2020), and increasing the use of renewable energy sources (Agathokleous and Kalogirou, 2016). However, the adoption of DSFs in Mediterranean climates, characterized by high temperatures and solar radiation (Vardopoulos et al., 2024b), has been limited due to concerns about increased solar heat gains and the potential for overheating (Vassiliades et al., 2022a).

1.2. Literature review

Energy-efficient retrofitting of buildings is a significant aspect of achieving sustainable development and mitigating climate change. Mediterranean countries, including Cyprus, Spain, Italy, and Greece, face a unique set of challenges due to their specific climate and building stock (Escrivà Saneugenio et al., 2024). A number of researchers stress the materiality impact on energy-efficient retrofitting in Mediterranean countries. Aranda *et al.* (2017) (Aranda et al., 2017) evaluated the environmental and economic impact of using locally sourced natural insulation materials in a renovation project in Spain. Their findings indicated that natural insulation materials could significantly reduce both the environmental impact and the cost of renovation. Similarly, Papadaki *et al.* (2019) (Papadaki et al., 2019) studied the materiality of two demo houses on the island of Crete, southern Greece, investigating the use of PCM. On the other hand, Chel and Kaushik (2018) (Chel and Kaushik, 2018) point out that utilizing locally accessible building materials with low embodied energy helps avoid using a lot of energy during construction, which lowers CO_2 emissions from the building sector. They stress that an energy-efficient building requires careful consideration of both passive and active design elements. Similarly, Scheinherrová *et al.* (2022) (Scheinherrová et al., 2022) investigate the practicability of repurposing fired clay brick waste, an unconventional by-product of brick manufacturing, to formulate gypsum-based binders endowed with enhanced water resistance. The outcomes disclosed in this research offer a potential avenue to mitigate the need for disposing of fired clay brick waste, transforming it into a valuable binder material suitable for eco-friendly applications in the rendering of buildings and the restoration of historical structures.

Gondal *et al.* (2021) (Gondal et al., 2021) have demonstrated that incorporating passive measures into the building envelope, either during construction or retrofitting, can reduce energy consumption without compromising occupants' comfort levels. Bhamare *et al.* (2019) (Bhamare et al., 2019) have emphasized the importance of considering local climatic conditions when designing passive techniques, as they can reduce cooling energy demand and overall energy consumption. Orientation has been identified as an important tool by Albatayneh *et al.* (2018) (Albatayneh et al., 2018) and Vassiliades *et al.* (2022) (Vassiliades et al., 2022b) for improving occupant comfort and reducing heating and cooling loads.

While passive measures are important for energy-efficient building design, other factors can also affect the success of energy renovations, including the local climate and active measures. Gustafsson *et al.* (2017)

(Gustafsson et al., 2017) found that energy efficiency measures can reduce final energy costs by up to 74 % in the Mediterranean climate, and such renovations have lower life cycle costs and environmental impacts compared to those without energy efficiency measures. Sheila Conejos *et al.* (2021) (Conejos et al., 2021) also note that while green energy technologies such as BIPV façade applications can be effective, issues with cost, aesthetics, and implementation can hinder their adoption. Inclusive energy renovations in the Mediterranean climate need to consider both passive and active systems to maintain indoor thermal conditions and reduce heating demand. Ochoa and Capeluto (2008) (Ochoa and Capeluto, 2008) agree, stating that combining both strategies can lead to consistent energy savings of 50–55 % while using either active or passive strategies alone can result in energy savings ranging from 8 % to 60 %. However, when renovating existing buildings (see for example (Tsilika and Vardopoulos, 2022)), space constraints pose a challenge, and both passive and active measures must be incorporated into the building envelope to achieve realistic results.

This study goes beyond the simple employing of passive and active strategies by examining the impact of DSFs and BIPV systems on the building's energy efficiency and feasibility. BIPV is a multi-functional technology that provides thermal insulation, shading, and electricity generation, leading to advances in architectural design and a reduction in carbon emissions. Several researchers have highlighted the benefits of BIPV, including its contribution to architectural design (Kang et al., 2019; Yang et al., 2018; Vassiliades et al., 2018) and carbon emissions reduction (Liu et al., 2021; Moreno et al., 2023; Charalambous et al., 2023).

According to Attoye *et al.* (2017) (Attoye et al., 2017), customization of conventional BIPV façades can improve their aesthetic and energy generation capabilities. Double-façade PV integration is also commonly used, as air flow in the cavity can enhance the PVs' cooling and efficiency (Vassiliades et al., 2022a). There is significant research into the effects of ventilation on BIPV performance (Peng et al., 2015, 2016a; Kundakci Koyunbaba and Yilmaz, 2012; Irshad et al., 2019; Shahrestani et al., 2017) as well as into the materials used in BIPV systems (Kant et al., 2020; Hasan et al., 2016; Čurpek and Čekon, 2020; Moreno et al., 2022) and bifacial systems (Tina et al., 2021; Assoa et al., 2021). Regarding the transparency of the façade, as per Peng *et al.* (2016) (Peng et al., 2016b), the use of semi-transparent PV modules in a BIPV DSF can result in a 50 % decrease in net electricity consumption.

Generally, DFs are an increasingly popular strategy for designing energy-efficient buildings, something that has also been parametrically investigated. The parametric approach to designing DFs involves using computer simulations to optimize the design parameters for energy efficiency, daylighting, thermal comfort, and other performance factors. This approach allows designers to explore a wide range of design options and quickly evaluate the impact of various design choices on the performance of the building.

Numerous studies have been conducted to investigate the use of the parametric approach in DF design. An example of a parametric approach in DSF design and investigation was conducted by Alberto *et al.* (2017) (Alberto et al., 2017). They evaluated the impact of various parameters, such as geometry, airflow path, cavity depth, opening area, and glazing type, on the performance of DSFs in a Mediterranean climate. Their findings indicated that the airflow path was the most crucial aspect in achieving an efficient DSF. The multi-story DSF was found to be the most efficient, reducing HVAC-related energy demands by approximately 30 %. Iken *et al.* (2019) (Iken et al., 2019) also used a parametric approach to investigate the impact of air cavity thickness on the behaviour of a smart DSF, which controls the greenhouse effect generation. Their results revealed that this smart configuration significantly reduced both heating and cooling loads. Lee *et al.* (2019) (Lee et al., 2019) proposed a PV DSF as a cost-effective method to enhance the performance of building envelopes. The PV DSF system was designed to be installed in both new and existing buildings, even while occupants were present. The optimal monthly operating angles of the PV vent window for minimizing heating and cooling energy demand were found to be the same as those for maximizing power generation. Proper operation of the PV vent window significantly reduced the energy demand of buildings. Barone *et al.* (2023) (Barone et al., 2023b) conducted a comparative analysis of a standard DF, a BIPV DF, and a BIPVT DF. Their findings reveal that the conventional DF system exhibits lower heating demand, but higher cooling needs compared to the other systems. Additionally, an augmentation in the cavity depth between the PV system and the façade led to elevated heating thermal loads and reduced cooling loads.

The literature review reveals that other researchers have thoroughly studied individual aspects of this research. The research gap lies in the combination of these aspects, which is what this study attempts to do. The use of DSFs is proposed as a necessary upgrade for the current building stock in the Mediterranean region. Building integrated solar systems supports this upgrade by providing renewable energy when the parametric approach is applied to identify the optimal combination of geometry, morphology, and materials.

1.3. Aim of the study

The current work aims to parametrically investigate the potential of DSFs with building-integrated active solar systems for energy renovation of buildings in the Mediterranean region. The novelty of the research lies in the fact that it pioneers a dynamic simulation model tailored for Mediterranean climates, addressing the intricacies of high temperatures and solar radiation. This innovative approach intricately considers solar radiation, thermal insulation, airflow dynamics, and the integration of active solar systems in DSFs. By aligning with the unique challenges of the Mediterranean, this study provides nuanced insights, surpassing generic solutions to contribute to region-specific retrofitting strategies. Additionally, adopting a parametric approach, this research offers fundamental design guidelines for energy renovations with DSFs and integrated solar systems. This proactive tool systematically explores configurations, bridging the gap between research and practical application, and enhancing accessibility to sustainable retrofitting solutions. Beyond a singular focus on energy metrics, the investigation delves into broader building performance aspects, including increased renewable energy utilization. This holistic perspective enriches the discourse on sustainable retrofitting, emphasizing multifaceted benefits for a comprehensive and resilient impact, when the findings of this study can contribute to the development of effective policies and strategies for sustainable building renovation in the region.

2. Material and methods

The methodology employed is based on dynamic simulations aimed at investigating the potential of DSFs with building-integrated active solar systems for energy renovation of buildings in the Mediterranean area. The research focuses on developing a comprehensive analysis using a well-established building energy performance simulation tool (BEPS) to account heat transfer phenomena through the building. Additionally, an in-house dynamic simulation tool, written in MatLab environment, assesses the airflow and temperature field occurring in the DSFs, as well as the energy performance of PV panels mounted on it. This approach is applied to a reference building, which represents the typical characteristics of buildings in a Mediterranean climate like Cyprus, to test different solutions related to DSFs. As said, the developed methodology exploits the potential of commercial software, such as TRNSYS and Google SketchUp, with the possibility of customizing the simulation with novel in-house tools written in MatLab environment. In Fig. 1, a conceptual study framework depicting the seven distinct steps of the employed methodology is presented. This diagram provides a concise overview of the key components of the employed methodology and their sequential relationships.

Firstly, the 3D geometrical model of the reference building is

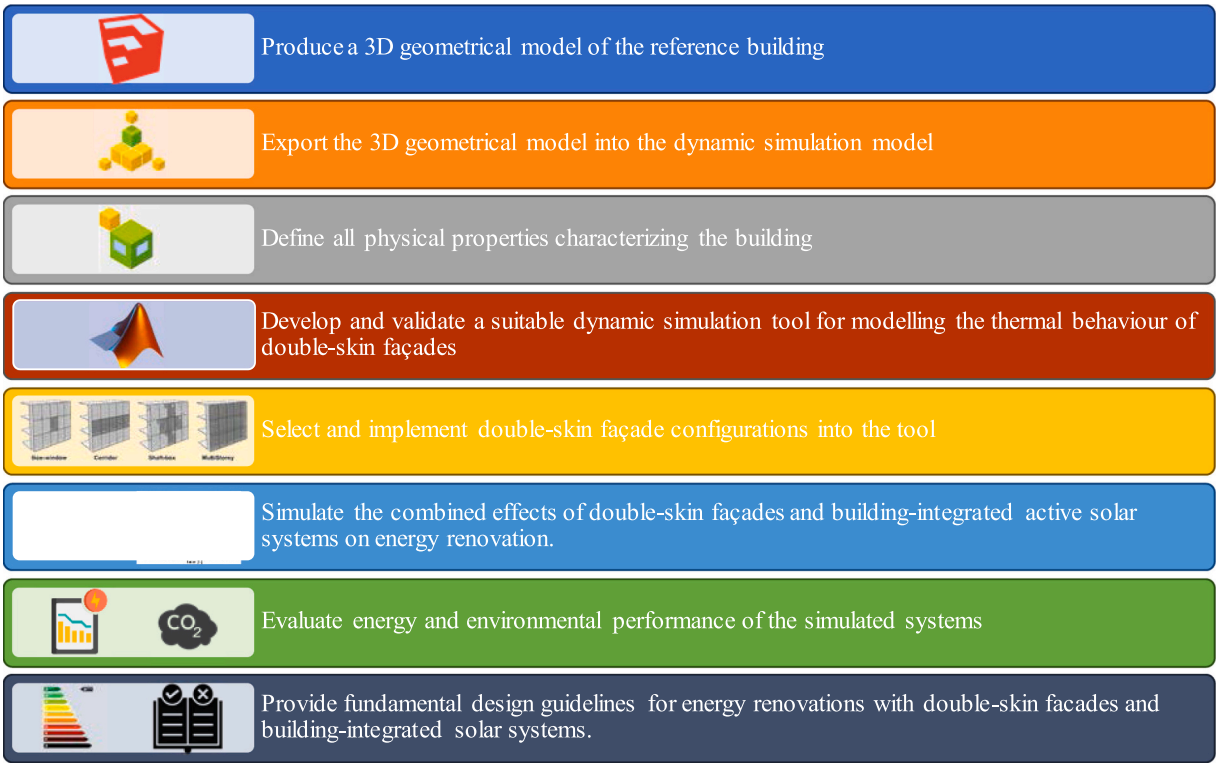

Fig. 1. Study conceptual framework of the methodology steps.

developed using the commercial software Google SketchUp (Schell and Esch, 1999), which enables an accurate representation of the shape and features of the building. During the 3D modelling phase, the TRNSYS3D tool (TRNSYS, 2019) is then utilized to select thermal zones within the building; this step is crucial for analysing the thermal behaviour of different areas within the building. The 3D geometrical model, along with the defined thermal zones, is subsequently implemented in the TRNSYS environment by using *type 56*, a suitable subroutine purposely designed for building energy simulations. In this phase, all thermo-physical parameters are defined and included into the simulation model to assess the energy performance of the reference building. Transient simulations are conducted within the TRNSYS environment to analyse the dynamic behaviour of the building and evaluate the effectiveness of various DSF configurations. Furthermore, to assess the energy performance of DSFs, an in-house subroutine is written in MatLab environment and linked to TRNSYS. Specifically, the development of this subroutine is needed because TRNSYS does not have any *type* that allows simulating the energy performance of DSF. Further details regarding the developed subroutine, together with an experimental verification, are provided in the next subsections. However, by this methodology, different simulations that consider factors such as solar radiation, thermal insulation properties, airflow, and the integration of active solar systems within the DSF are conducted. The main objective of this research is to investigate the combined effects of DSF and building-integrated active solar systems on the energy renovation of buildings in the Mediterranean region. Moreover, a parametric approach is also employed to provide fundamental design guidelines for energy renovations utilizing DSFs with building-integrated solar systems. It also sheds light on the benefits and challenges of implementing this technology in the context of the Mediterranean climate. By focusing on the aging building stock in Europe, this research aims to contribute to the development of energy-saving solutions.

2.1. *Dynamic simulation model*

To evaluate the energy performance of DSF, an in-house dynamic simulation tool has been developed in MatLab environment (MATLAB, 1984). Subsequently, it has been integrated into the commercial TRNSYS software by using *type 155* (Yesilyurt et al., 2023). This approach facilitates the adoption of the capabilities of TRNSYS software, a validated and certified building energy performance simulation tool renowned for its efficacy in conducting comprehensive energy analyses of buildings (Sun et al., 2017), and the flexibility of implementing its suitable simulation tools. Moreover, TRNSYS offers the flexibility to accommodate bespoke tools, thereby enabling the consideration of emerging technologies and their impact on building energy performance. The developed tool is based on a suitable resistive-capacitive thermal network and allows for simulating DSF, as reported in Fig. 2.

The tool is designed to simulate DSF, such as the one depicted in Fig. 2*a*. Here, it illustrates the working principle of the DSF: outdoor fresh air is drawn from the outside, facilitating natural ventilation and stack effects. This process aids in cooling the PV panels and influences the heat exchange phenomenon occurring through the external walls of the building. The TRNSYS software can conduct energy performance analysis on multizone buildings through the adoption of *type 56*. Specifically, this component simulates the thermal behaviour of buildings divided into multiple thermal zones, and it includes as input thermal and optical data for windows, materials and thicknesses of the vertical and horizontal opaque surfaces, convective heat transfer coefficients, and a weighting factor for calculating operative room temperature. Thus, a customised tool based on a resistive-capacitive thermal network is developed and embedded in the TRNSYS environment through *type 155*. Specifically, this type allows for establishing a link between MatLab and TRNSYS and communicating with the in-house-developed tool. The main output of the developed tool is the temperature field of the air flow flowing into the gap cavity along the z-coordinate. The following differential equation is included in the tool:

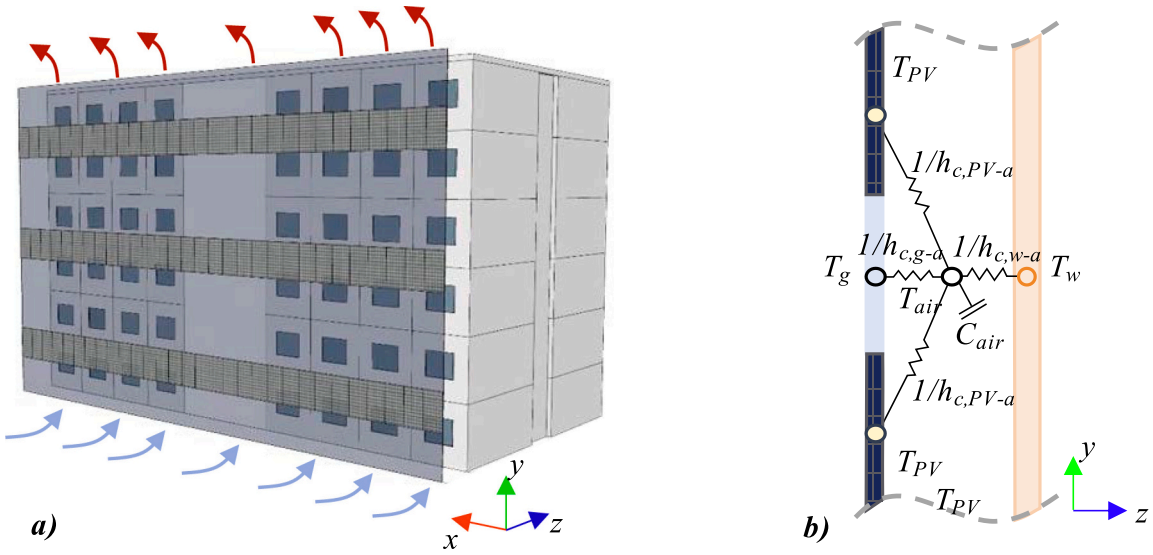

Fig. 2. Double skin façade: *a)* working principle; *b)* resistive-capacitive thermal network.

$$\rho c V \frac{dT_{air}}{d\theta} = D \cdot dy \left[h_{c,PV-a}(T_{PV} - T_{air}) + h_{c,g-a}(T_g - T_{air}) + h_{c,w-a}(T_w - T_{air}) \right] \quad (1)$$

where ρ is the density of the air flow, c is the specific heat, V is the sub-volume in which the air channel included between the PV façade and the conventional external wall is divided, T_{air} is the temperature field of the air flow flowing into the gap cavity, θ is the timestep of the simulation, D is the depth of the gap cavity along the z-coordinate, dy is the infinitesimal height of the discretized wall composing the façade, $h_{c,PV-a}$ is the convective heat transfer coefficient between the PV panels included into the DSF and the air flow, T_{PV} is the temperature of the PV cell, $h_{c,g-a}$ is the convective heat transfer coefficient between the glass cover included in the DSF and the air flow, T_g is the temperature of the glass cover, $h_{c,w-a}$ is the convective heat transfer coefficient between the wall of the building and the air flow, and T_w is the temperature of the external wall of the building. Therefore, the tool is embedded in the TRNSYS environment according to the layout reported in Fig. 3.

Here, the light blue dashed lines represent the weather boundary condition parameters, the dark blue dashed lines represent the input parameters of the modelled DSF, and the green dotted lines represent the output results. Additionally, other types involving the weather data file implementation, the building physics parameters, and the MatLab icon are also clearly visible. All these *types* represent the developed co-simulative tool that embeds the mathematical model of the DSF tool with the BEPS commercial software.

2.2. Experimental verification

To assess the reliability of the developed procedure, the simulated results are compared with experimental data available in the scientific literature. Numerous experimental analyses on DSFs are available; however, two different climatic conditions are selected for testing the reliability of the model. The studies adopted for the experimental validation procedure involve two different DSFs with varying depths of air cavities (Wu et al., 2022; Dama et al., 2017). The in-house developed tool is configured to replicate the same conditions of the DSFs studied in these papers, including the external boundary conditions. To numerically quantify the goodness of the developed model, five different parameters are selected. These parameters are the follow: mean error (*ME*), mean absolute error (*MAE*), mean average percentage error (*MAPE*), root mean square error (*RMSE*), and standard deviation (σ). These parameters are assessed according the Eqs.(2)-(6), and the mathematical formulations are the follow:

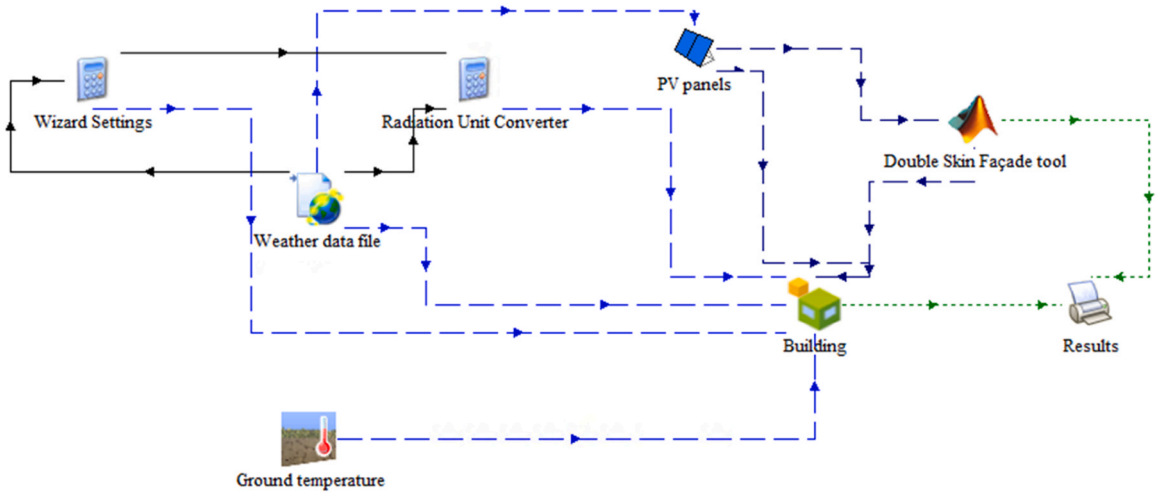

Fig. 3. Implementation into the building energy performance simulation tool environment.

$$ME = \frac{1}{n}\sum_{i=1}^{n}(A_i - F_i) \quad (2)$$

$$MAE = \frac{1}{n}\sum_{i=1}^{n}|A_i - F_i| \quad (3)$$

$$MAPE = \frac{1}{n}\sum_{i=1}^{n}\left|\frac{A_i - F_i}{A_i}\right| \cdot 100 \quad (4)$$

$$RMSE = \sqrt{\frac{1}{n}\sum_{i=1}^{n}(F_i - A_i)^2} \quad (5)$$

$$\sigma = \sqrt{\frac{1}{n}\sum_{i=1}^{n}(F_i - \mu)^2} \quad (6)$$

where n is the number of simulated data, A_i is the experimental data to be compared to the simulated data, F_i is the simulated data, and μ is the experimental data mean value.

As preliminary said, the dataset A_i is gathered from the experimental results provided by (Wu et al., 2022; Dama et al., 2017). Specifically, for the reference (Wu et al., 2022) 188 experimental points is considered, whereases for the reference (Dama et al., 2017) 288 experimental points are considered. Therefore, the experimental verification is conducted for a dataset population of approximately 476 experimental points. For the sake of brevity, the experimental hourly profile of the outlet airflow temperature is compared with the simulated results for a sample day of the experimental campaign reported in (Wu et al., 2022). This comparison is shown in Fig. 4.

Specifically, the blue scattered plot represents the simulated results, while the grey scattered plot represents the experimental data provided in (Wu et al., 2022). Note that suitable error bars indicating ±5 % for the experimental data are included in the figure.

From this figure, it is possible to see that the developed DSF model integrated into the BEPS tool follows the trend of the experimental results with very good agreement. Similar agreements are obtained for the experimental verification conducted for the comparison with the reference (Dama et al., 2017), however, for the sake of brevity, the hourly trends for these results are not reported. Instead, to show the whole results of the experimental verification, Fig. 5 presents two graphs involving the two considered works, illustrating the comparison between the simulated and experimental temperatures.

From these figures it is possible to see that for both experimental datasets, the simulated results are always in the range ±15 %. Specifically, for Wu et al. (2022), the comparison reported in the left side of Fig. 5, a *ME* about −0.16°C, a *MAE* of 0.57°C, a *MAPE* of 2.62 %, a *RMSE* about 0.657, and a σ is about 0.64. Furthermore, for Dama et al (Dama et al., 2017)., the comparison reported in the right side of Fig. 5, a *ME* about −0.25°C, a *MAE* of 0.96°C, a *MAPE* of 6.24 %, a *RMSE* about 1.18, and a σ is about 1.16.

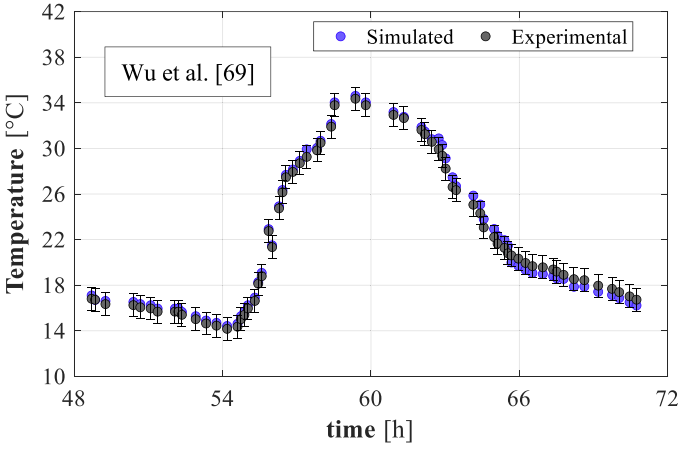

Fig. 4. Hourly comparison between the experimental and simulated data for the experimental validation procedure.

2.3. Proof-of-concept

The analysis conducted refers to a three-story building positioned with its long side facing east to west. A reference building is modelled by using the commercial software Google SketchUp to study the impact of various DSFs. The Trnsys3D plugin is employed to develop a three-dimensional model of the reference building and export it to the TRNSYS environment. Simulations are performed for the entire building, with a specific focus on sample thermal zones. The reference building is divided into 25 thermal zones. These zones comprised 24 air-conditioned areas with two different temperature and relative humidity setpoints: 20°C and 50 % for the winter season, and 26°C and 60 % for the summer season. The thermal zones are open office spaces, and the heating and cooling systems are scheduled to operate from 08:00–18:00 during weekdays, while one thermal zone operates in a free-floating mode. Fig. 6 illustrates a sketch of the simulated reference building.

The overall dimensions of the building are 30 m in length, 14 m in width, and 18 m in height. Each air-conditioned thermal zone measured 12 m in length, 6 m in width, and 3 m in height. Additionally, each thermal zone is equipped with four windows measuring approximately 1.5 m × 1.2 m. The building walls have a thickness of 30 cm and a U-value of 1.813 W/(m^2·K), while the floor/ceiling has a thickness of 14 cm and a U-value of 2.14 W/(m^2·K). The wall composition consisted of concrete (with thermal conductivity of k = 1.13 W/(m·K), density of ρ = 1400 kg/m^3, and specific heat capacity of c = 280 J/(kg·K) and thermal insulation (with thermal conductivity of k = 0.034 W/(m·K), density of ρ = 14.0 kg/m^3, and specific heat capacity of c = 1050 J/(kg·K)). The opaque external surfaces have an absorptance of 0.6. Solar radiation penetrated the windows and affected the internal zones, assuming absorption coefficients of 0.40 for both the floor and the interior walls. The glazing consisted of a double-glazed system with air in between the panes, measuring 4–16–4 in thickness. The U-value for the glazing was 1.06 W/(m^2·K), and the SHGC is 0.5, simulating a translucent surface to diffuse transmitted light and prevent glare discomfort. Note that, as mentioned in the previous paragraph, this study focuses on the aged building stock of the Mediterranean region. Therefore, high U-values for opaque and transparent surfaces represent old buildings that do not comply with the regulation limit values. For these thermal zones, which are considered apartments, a ventilation rate of 0.5 air changes per hour and a crowding index of 0.10 persons per square meter are assumed. The internal thermal loads included people (at 95 W/person), lighting, and equipment (totalling 25.0 W/m^2). The reference building is climatized using air-to-water electric heat pumps/chillers, sized based on the maximum load, supplying hot and cold water to a fan-coil system with a COP of about 4.5 for heating mode and 5.0 for cooling mode. The present study introduces a novel architectural system comprising a DSF distinguished by the integration of monocrystalline PV panels and double-glazed glass elements. The investigation is grounded in the examination of two distinct system configurations, both of which are meticulously depicted in Fig. 7.

In Fig. 7, the schematic representation of the proposed system layout is delineated, with the left side illustrating the half DSF configuration and the right side depicting the full DSF configuration. These conceptual frameworks are distinguished by their respective panel-to-glass surface ratios and the associated quantities of PV panels. In the half-DSF configuration, 75 PV panels are arrayed in three rows, encompassing approximately 30 % of the façade, resulting in a PV-to-Glass ratio of approximately 0.43. Conversely, the full DSF configuration incorporates 150 PV panels arranged in six rows, covering approximately 60 % of the façade, yielding a PV-to-Glass ratio of approximately 1.50. Furthermore, our analysis extends to the influence of the separation distance between the building façade and the DSF structure. To achieve this objective, we conducted simulations using two different quantities of PV panels (*i.e.*,

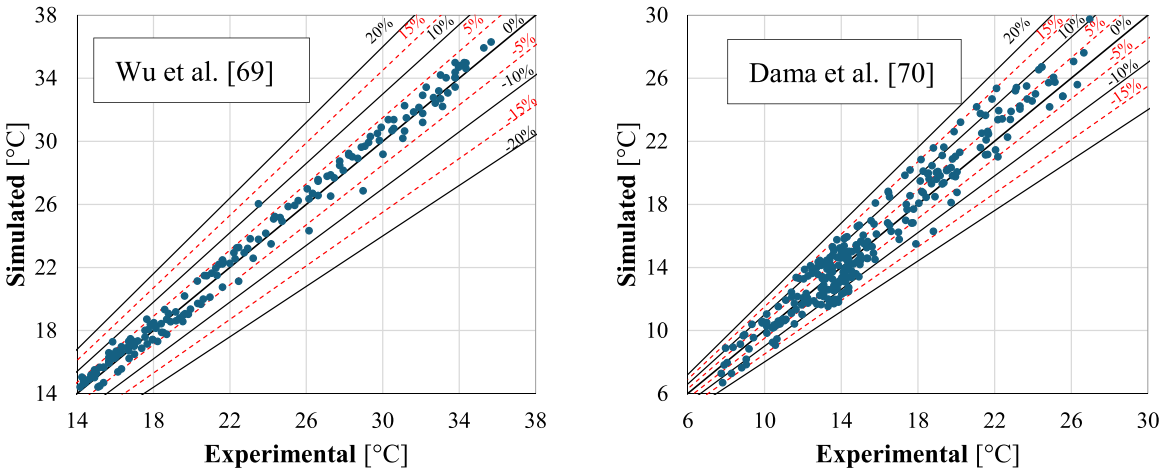

Fig. 5. Experimental vs. Simulated outlet temperature for the two considered scientific works.

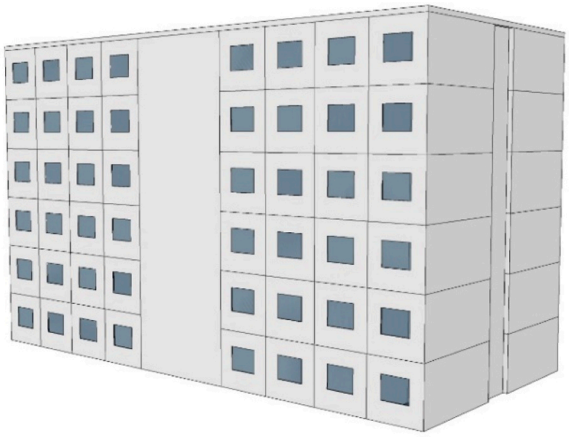

Fig. 6. Reference building.

75 and 150) and explored eleven distinct depth dimensions of the DSF gap, ranging from 0.5 to 10.0 m. All the PV panels adopted in this study are monocrystalline solar panels, with a nominal efficiency of about 21 %. A summary of the investigated system layouts is presented in Table 1. Simulations were conducted utilizing a time step of 6 minutes over a standard solar year for the weather zone of Nicosia (CY) based on the adopted Typical Meteorological Year (TMY) dataset. As noted above, eleven distinct depth dimensions of the DSF gap were explored, ranging from 0.5 to 10.0 m. The primary objective was to evaluate the potential of different gap sizes as architectural solutions, including their use as semi-covered verandas or other functional spaces. The larger gaps, can serve practical purposes in architectural design, providing additional semi-open spaces that enhance the usability of buildings (Barone et al., 2023b).

The use the commercial simulation tools, while powerful, may limit the replicability of the methodology for researchers who do not have access to these software packages. As such, this reliance on licensed software is acknowledged as a limitation of the study. To facilitate the reproducibility of the methodology, a supplementary file is provided, the MATLAB script developed for coupling the calculations with the

Table 1
Investigated system layouts.

Layout	N PV Panels	Depth	Layout	N PV Panels	Depth
[-]	[-]	[m]	[-]	[-]	[m]
REF	0	-			
PRO 1	75	0.5	***PRO 12***	150	0.5
PRO 2	75	1.0	***PRO 13***	150	1.0
PRO 3	75	2.0	***PRO 14***	150	2.0
PRO 4	75	3.0	***PRO 15***	150	3.0
PRO 5	75	4.0	***PRO 16***	150	4.0
PRO 6	75	5.0	***PRO 17***	150	5.0
PRO 7	75	6.0	***PRO 18***	150	6.0
PRO 8	75	7.0	***PRO 19***	150	7.0
PRO 9	75	8.0	***PRO 20***	150	8.0
PRO 10	75	9.0	***PRO 21***	150	9.0
PRO 11	75	10	***PRO 22***	150	10

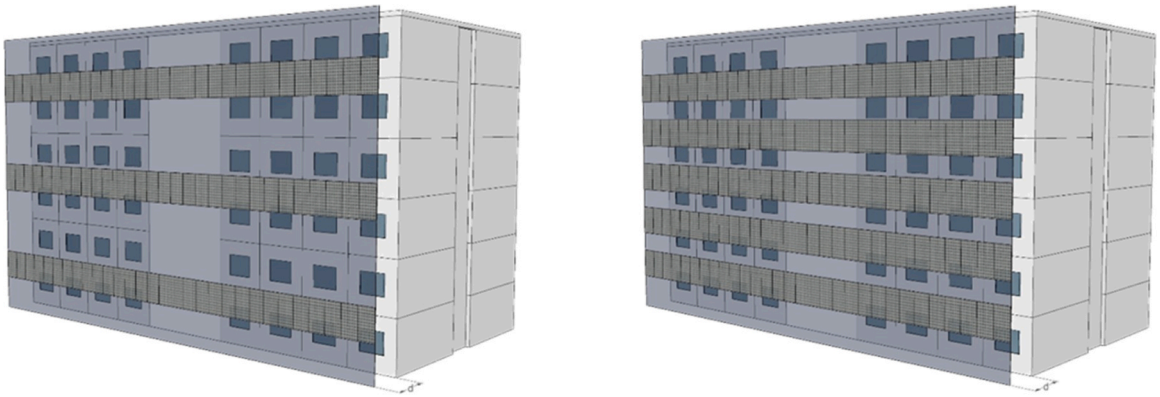

Fig. 7. Proposed DSF: left) half DSF, right) full DSF.

TRNSYS software. This script allows other researchers to replicate the analysis and adapt it to their specific contexts, provided they have access to the required commercial software.

3. Results and discussion

Within this section, we provide a comprehensive exposition of the outcomes derived from the DSF systems, encompassing results on an hourly, monthly, and annual basis. For conciseness, our focus on hourly results narrows down to two specific instances: firstly, during the initial 168 hours corresponding to the winter season (*i.e.*, from January 1st to January 7th), and secondly, during select summer weeks (from 4824th to 4992nd, corresponding to July 19th to July 26th). These timeframes have been chosen due to their representation of worst-case scenarios for both heating and cooling demands. Our analysis concentrates solely on the first eleven system configurations, each equipped with 75 PV panels. It is imperative to acknowledge that equivalent assessments have been conducted for the remaining eleven system layouts, characterized by the presence of 150 PV panels, thereby ensuring a comprehensive exploration of the performance spectrum.

Fig. 8 illustrates the temperature distribution profiles of various components incorporated within the façade structure, pertaining to two representative weeks during the winter and summer seasons. The blue solid line refers to the outdoor dry-bulb temperature, the solid orange line represents the temperature of the PV panels included in the DSF, the yellow solid line depicts the temperature of the glass included in the DSF, and the solid violet line shows the temperature of the air gap between the DSF and the external wall of the building.

These findings are based on the PRO 1 system configuration, characterized by a DSF depth of approximately 0.5 meters. The thermal dynamics of the system are succinctly encapsulated within this visual representation, indicating the functioning of the system as a BIPV/T system. Notably, the system's efficient performance is attributed to the minimal separation distance between the two façade layers, which facilitates the attainment of elevated air gap temperatures in close proximity to the PV panels and glass covering. Specifically, the temperature profile of the PV panels exhibits the highest thermal levels, with a peak temperature reaching approximately 38°C during the representative winter week and around 65°C during the analogous summer week. Subsequently, the second highest temperature reading corresponds to the glass covers, which constitute the remaining component of the DSF system. Following this, the third temperature parameter pertains to the air gap temperature, situated between the temperature of the glass cover and the ambient air temperature. It is imperative to note that this phenomenon is intricately tied to the depth of the gap and the corresponding quantity of PV panels. A visual representation elucidating the initial assertion is provided in Fig. 9.

Fig. 10 presents the outcomes of the parametric investigation, elucidating the temperature dynamics within the air gap cavity in conjunction with ambient air temperature variations. Notably, this analysis encompasses DSF depths of the air gap of 0.5 meters (PRO 1), 5.0 m (PRO 6), and 10.0 m (PRO 11). It becomes apparent that distinct and discernible air gap temperature profiles emerge for PRO 1, PRO 6, and PRO 11, with PRO 11 displaying the most subdued air gap temperature trend. These divergent temperature trends subsequently give rise to varying thermal loads, as illustrated in Fig. 11.

Across all three examined system configurations, discernible trends are evident: an increase in the depth of the air gap cavity corresponds to higher heating loads while conversely leading to reduced cooling loads. This phenomenon arises from the expanded depth of the air channel, facilitating enhanced heat dissipation from the building, consequently elevating heating demands and reducing cooling requirements. For the three selected winter days, it is observed that the reference case necessitates a total heating energy input of approximately 642 kWh. Notably, the lowest heating demand is recorded for PRO 1, aligning with its lower air gap temperature profile, amounting to 611 kWh (a reduction of 4.82 % compared to the reference case). Additionally, PRO 6 also exhibits reduced heating requirements compared to the reference case, registering 629 kWh (a decrease of 2.02 %).

Conversely, PRO 11 displays higher heating needs than the reference case, reaching 651 kWh (a rise of 1.66 %). Conversely, dissimilar trends manifest for cooling demands: the reference case demands approximately 7.61 MWh for cooling, while the lowest cooling requirement is observed for PRO 11, coinciding with its elevated air gap temperature profile, accounting for 7.29 MWh (a reduction of 4.02 %). In contrast, both PRO 1 and PRO 6 necessitate higher cooling loads than the reference case, with values of 8.10 MWh (an increase of 6.05 %) and 7.70 MWh (an increase of 2.02 %), respectively, for PRO 6. These results mirror the annual findings, as depicted in Fig. 11.

In the context of heating requirements, it becomes evident that a small DSF configuration is the favoured choice when the objective is the minimization of heating demands. More specifically, opting for a DSF with a depth of less than 7.0 m yields a reduction in heating demands ranging from −5.49 % to −0.82 % is achievable. Conversely, inverse considerations apply when contemplating cooling loads: a substantial DSF configuration is the preferred option when the aim is to reduce cooling requirements. To be precise, selecting a DSF with a depth exceeding 6.0 m facilitates a reduction in cooling loads. The depth of the air gap cavity also reflects on the electricity production of the PV panels implemented in the DSF, as reported in Fig. 12 and Fig. 13.

Fig. 12 illustrates the electricity generation associated with varying depths of the DSF. Consistent with expectations, a direct relationship is observed, whereby an increased depth of the air gap cavity leads to enhanced electrical efficiency of the PV panel, consequently resulting in higher electricity production from the PV panels. In this instance, at the 4932nd hour, it is discerned that the electrical power output is

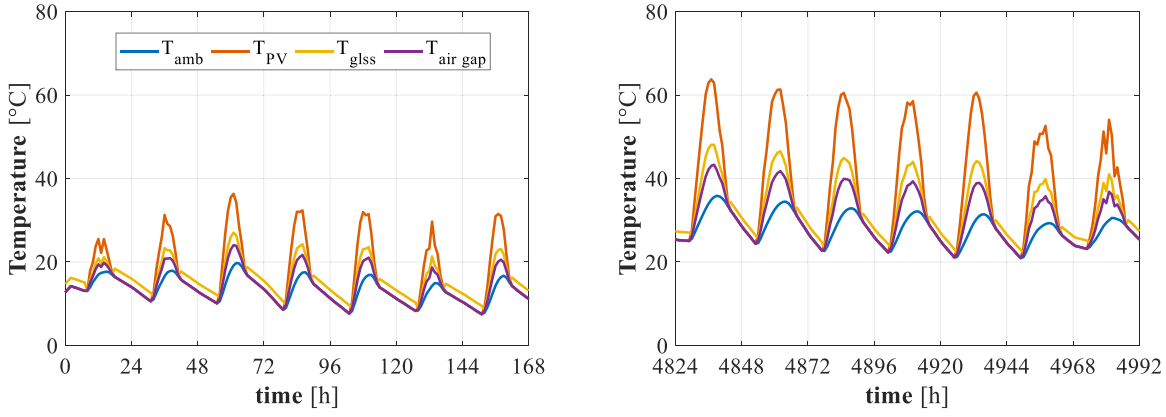

Fig. 8. Temperature distribution along the DSF system for two sample weeks.

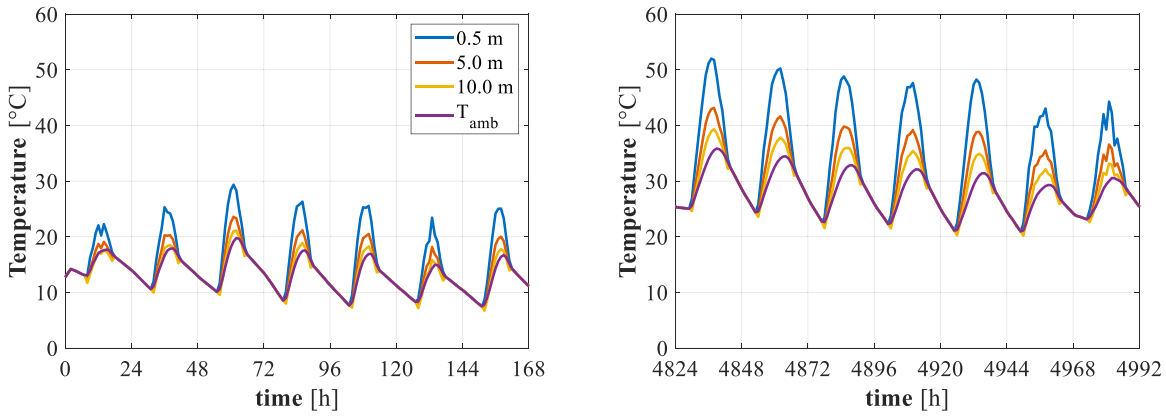

Fig. 9. Airflow temperature for different depths of the air gap of the DSF (0.5 m - PRO 1, 5 m - PRO 6, and 10 m - PRO 11).

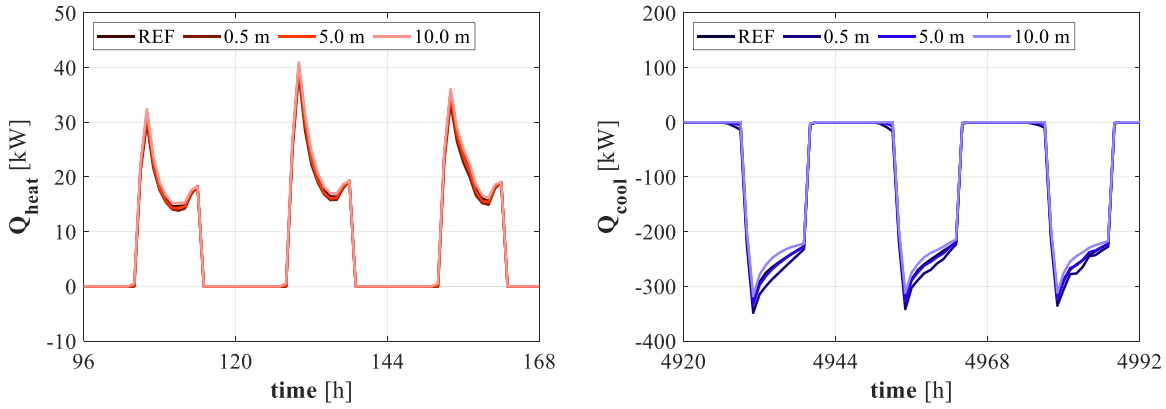

Fig. 10. Hourly thermal loads for three sample winter (left) and summer (right) days for different DSF depths of the air gap (0.5 m - PRO 1, 5 m - PRO 6, and 10 m - PRO 11).

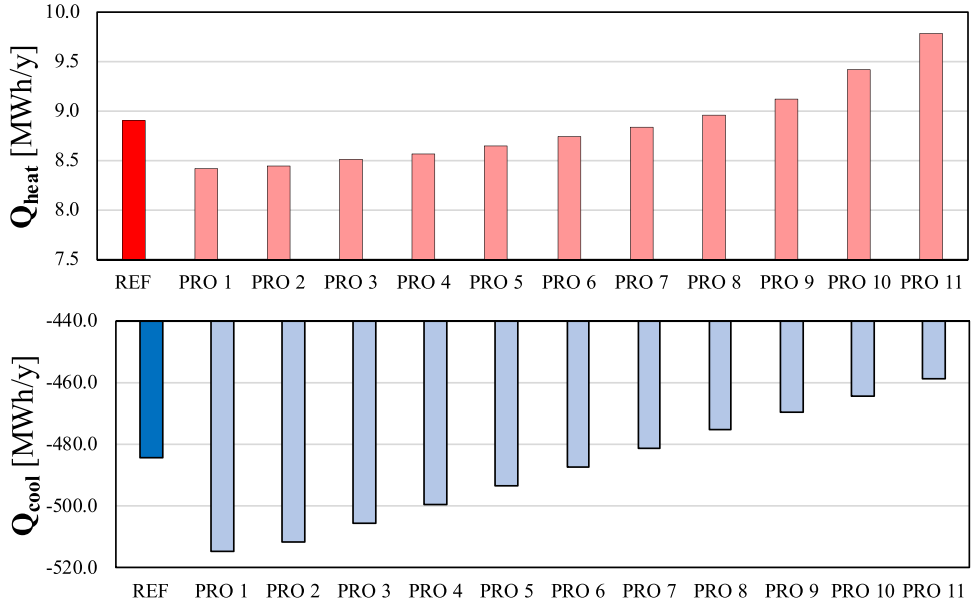

Fig. 11. Yearly heating and cooling trends for the first eleven proposed system layouts.

approximately 19.5 kW for the smallest cavity depth, 20.7 kW for a depth of 5.0 m, and reaches its peak at approximately 21.3 kW for the greatest cavity depth. This observed phenomenon underscores the influence of the DSF depth of the air gap on electrical performance and can also be seen in the yearly electricity production, as reported in Fig. 13.

In this figure, it is possible to notice a trend similar to the heating needs. Specifically, as seen in the previous figure, the higher the depth of the air captivity, the higher the cooling effects on the PV panels, and

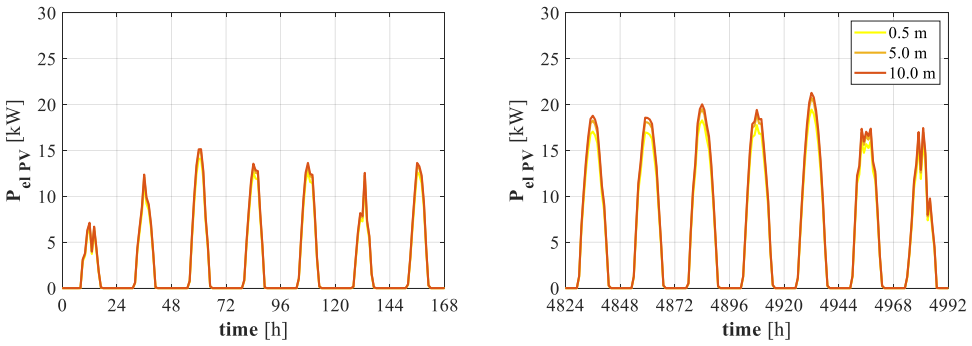

Fig. 12. Electricity production for different DSF depths of the air gap (0.5 m - PRO 1, 5 m - PRO 6, and 10 m - PRO 11).

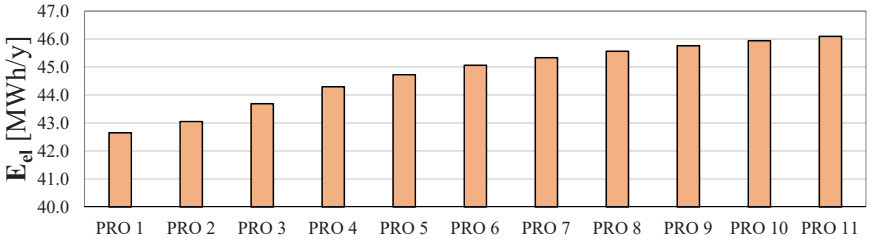

Fig. 13. Yearly electricity production trends for the first eleven proposed system layouts.

consequently, the higher the electricity production is achievable.

To summarize the results obtained in terms of yearly heating and cooling needs, electricity demand due to heating and cooling, electricity production, net electricity demand, primary energy, primary energy savings, and carbon monoxide gas emissions are reported in Table 2.

The results obtained from the comprehensive analysis of DSFs with integrated solar active systems offer valuable insights with broader implications beyond the specific context of Mediterranean countries. While the study focuses on the Mediterranean region, where cooling demands are significant, the findings hold relevance for diverse climatic zones and building typologies. The observed trends in heating and cooling loads in response to DSF configurations, particularly the influence of air gap depth on thermal performance, are indicative of potential energy-saving strategies applicable in various geographical locations. For instance, the preference for smaller DSF configurations (<7.0 m depth) to minimize heating demands aligns with principles of energy-efficient design that prioritize insulation and thermal management. Conversely, the advantage of larger DSF configurations (>6.0 m depth) in reducing cooling requirements underscores the potential for passive cooling solutions in regions with high cooling loads. Additionally, the relationship between air gap depth and electricity production from PV panels highlights the significance of DSF design in optimizing renewable energy generation. While specific outcomes may vary depending on factors such as building orientation, opaque-transparent ratio of the DSF, occupancy patterns, and local climate conditions, the fundamental principles elucidated in this study provide a framework for designing

Table 2
Energy and environmental yearly results.

Conf.	Depth	Qheat		Qcool		$E_{el,demand}$	$E_{el,prod}$	$E_{el,demand,net}$	PE	PES	mCO2
	[m]	[MWh/y]	[%]	[MWh/y]	[%]	[MWh/y]	[MWh/y]	[MWh/y]	[MWh/y]	[%]	[t_{CO2}/y]
REF	0	8.91	-	−484.62	-	98.9	-	98.9	247.26		39.96
PRO 1	0.5	8.42	−5.49	−514.98	6.26	104.9	42.65	62.22	155.54		25.14
PRO 2	1.0	8.45	−5.19	−511.87	5.62	104.3	43.05	61.60	154.00	-37.1	24.89
PRO 3	2.0	8.51	−4.55	−505.68	4.35	103.0	43.69	59.34	148.35	−37.7	23.97
PRO 4	3.0	8.57	−3.81	−499.53	3.08	101.8	44.29	57.52	143.79	−40.0	23.24
PRO 5	4.0	8.65	−2.95	−493.43	1.82	100.6	44.72	55.88	139.71	−41.8	22.58
PRO 6	5.0	8.74	−1.97	−487.38	0.57	99.4	45.06	54.36	135.90	−43.5	21.96
PRO 7	6.0	8.84	−0.82	−481.39	−0.67	98.2	45.33	52.91	132.28	−46.5	21.38
PRO 8	7.0	8.96	0.57	−475.48	−1.89	97.1	45.56	51.53	128.82	−47.9	20.82
PRO 9	8.0	9.13	2.41	−469.77	−3.06	96.0	45.76	50.22	125.55	−49.2	20.29
PRO 10	9.0	9.42	5.72	−464.28	−4.20	94.9	45.94	49.01	122.53	−50.4	19.80
PRO 11	10	9.79	9.89	−458.80	−5.33	93.9	46.10	47.84	119.60	−51.6	19.33
PRO 12	0.5	8.35	−6.27	−526.01	8.54	107.1	82.41	24.65	61.62	−75.1	9.96
PRO 13	1.0	8.38	−5.98	−522.32	7.78	106.3	83.21	23.92	59.79	−75.8	9.66
PRO 14	2.0	8.44	−5.34	−514.96	6.26	104.9	84.48	20.38	50.96	−79.4	8.24
PRO 15	3.0	8.50	−4.59	−507.63	4.75	103.4	85.70	17.72	44.30	−82.1	7.16
PRO 16	4.0	8.58	−3.71	−500.35	3.25	102.0	86.56	15.42	38.55	−84.4	6.23
PRO 17	5.0	8.67	−2.70	−493.12	1.75	100.6	87.22	13.33	33.32	−86.5	5.38
PRO 18	6.0	8.78	−1.51	−485.95	0.27	99.1	87.77	11.37	28.43	−88.5	4.59
PRO 19	7.0	8.91	−0.07	−478.85	−1.19	97.8	88.23	9.52	23.80	−90.4	3.85
PRO 20	8.0	9.07	1.77	−471.94	−2.62	96.4	88.63	7.77	19.44	−92.1	3.14
PRO 21	9.0	9.36	5.02	−465.33	−3.98	95.1	88.98	6.16	15.41	−93.8	2.49
PRO 22	10	9.79	9.89	−458.80	−5.33	93.9	89.30	4.64	11.60	−95.3	1.87

energy-efficient building envelopes with DSFs. By extrapolating these findings to diverse contexts and building scenarios, policymakers, architects, and building professionals can leverage passive design strategies to enhance energy performance and sustainability across different regions and building types.

4. Conclusions

This study has delved into the pivotal intersection of climate change mitigation, energy efficiency, and building retrofitting, with a specific focus on the Mediterranean region. The building sector, being a major contributor to global energy consumption and greenhouse gas emissions, necessitates rigorous efforts to minimize its environmental impact. In this context, the incorporation of DSFs integrated with active solar systems emerges as a promising strategy for enhancing the energy performance of existing buildings.

The investigation undertaken here has leveraged parametric analysis, utilizing TRNSYS and MatLab software tools, to comprehensively explore the potential of DSFs with integrated solar active systems in Mediterranean countries. The results elucidate several critical insights that can guide sustainable building renovation practices in the region.

Firstly, the study has demonstrated that DSFs can be instrumental in reducing energy consumption for heating in multi-story existing buildings. Particularly, a smaller DSF depth of the air gap, such as the one with a dimension less than 7.0 m, proves to be advantageous in minimizing heating demands, yielding reductions ranging from −5.49 % to −0.82 %.

Conversely, when addressing cooling loads, the research underscores the advantage of larger DSF configurations. DSFs with a depth exceeding 6.0 m are shown to effectively mitigate cooling requirements, thereby offering the potential for energy-efficient cooling solutions.

Furthermore, the depth of the air gap cavity within the DSF significantly influences the electrical performance of integrated PV panels. An increase in the depth of the air gap is correlated with enhanced PV panel efficiency, resulting in higher electricity production. This phenomenon has been quantified, with yearly electricicity outputs varying from approximately 42.6 MWh/y for the smallest cavity depth to a peak of around 46.1 MWh/y for the greatest depth, emphasizing the impact of DSF design on electrical energy generation.

In a broader context, these findings emphasize the importance of tailored retrofitting solutions that consider local climate conditions and building characteristics when pursuing sustainable building renovations. Larger DSF gaps, while unconventional, are explored here for their potential architectural benefits, including the creation of semi-covered verandas. These solutions are particularly relevant in Mediterranean climates where outdoor living spaces are valued. The feasibility of constructing such gaps is contingent on specific architectural and engineering considerations, which are beyond the scope of this study but are acknowledged as an important aspect of practical implementation. Such considerations are pivotal in optimizing energy performance and reducing the carbon footprint of existing building stock in Mediterranean countries.

Additionally, the study underscores the importance of considering the specific dimensions and characteristics of building façades when implementing DSFs with integrated solar systems for optimal energy-efficient renovation. While the parametric analysis has provided crucial insights into the depth of DSFs and their impact on energy consumption, it becomes evident that the width and detailed configuration of the façade are equally critical factors in achieving sustainability goals. Future research and practical applications should delve into determining the most suitable width and design details of DSFs, aligning with the unique context of each building. This nuanced approach ensures a comprehensive retrofitting strategy that not only minimizes energy consumption but also integrates seamlessly with the diverse architectural and climatic features of Mediterranean buildings. As we advance towards more sustainable building practices, the consideration of façade width and specifics becomes integral to a tailored and effective approach to energy-efficient renovation.

In summary, the results obtained in this study encompass a spectrum of critical parameters, including yearly heating and cooling needs, electricity demand due to heating and cooling, electricity production, net electricity demand, primary energy consumption, primary energy savings, and carbon monoxide emissions. These outcomes collectively provide valuable insights that can inform policy development and strategy formulation for sustainable building renovation practices in Mediterranean countries. This research contributes to the ongoing discourse on climate change mitigation and energy efficiency within the building sector, underscoring the significance of context-specific solutions in advancing sustainability goals.

Declaration of Competing Interest

The authors declare that they have no known competing financial interests or personal relationships that could have appeared to influence the work reported in this paper

Data Availability

Data will be made available on request.

References

Agathokleous, R.A., Kalogirou, S.A., 2016. Double skin facades (DSF) and building integrated photovoltaics (BIPV): a review of configurations and heat transfer characteristics. Renew. Energy 89, 743–756. https://doi.org/10.1016/j.renene.2015.12.043.

Albatayneh, A., Alterman, D., Page, A., Moghtaderi, B., 2018. The significance of the orientation on the overall buildings thermal performance-case study in Australia. in: Energy Procedia. Elsevier Ltd, pp. 372–377. https://doi.org/10.1016/j.egypro.2018.09.159.

Alberto, A., Ramos, N.M.M., Almeida, R.M.S.F., 2017. Parametric study of double-skin facades performance in mild climate countries. J. Build. Eng. 12, 87–98. https://doi.org/10.1016/J.JOBE.2017.05.013.

Anon, 2009. The 2020 climate and energy package. Eur. Comm. Clim. Action. ⟨http://ec.europa.eu/clima/policies/package/index_en.htm⟩ (accessed June 1, 2015).

Aranda, J., Zabalza, I., Conserva, A., Millán, G., 2017. Analysis of energy efficiency measures and retrofitting solutions for social housing buildings in spain as a way to mitigate energy poverty, 2017, Vol. 9, Page 1869 Sustain 9, 1869. https://doi.org/10.3390/SU9101869.

Asdrubali, F., Guattari, C., Roncone, M., Baldinelli, G., Gul, E., Piselli, C., Pisello, A.L., Presciutti, A., Bianchi, F., Pompei, L., Mattoni, B., Bisegna, F., Kolokotsa, D., Tsekeri, E., Assimakopoulos, M.N., Efthymiou, C., Barmparesos, N., Lechowska, A., Schnotale, J., Aletta, F., Berardi, U., 2022. A Round Robin Test on the dynamic simulation and the LEED protocol evaluation of a green building. Sustain. Cities Soc. 78, 103654 https://doi.org/10.1016/J.SCS.2021.103654.

Assoa, Y.B., Thony, P., Messaoudi, P., Schmitt, E., Bizzini, O., Gelibert, S., Therme, D., Rudy, J., Chabuel, F., 2021. Study of a building integrated bifacial photovoltaic facade. Sol. Energy 227, 497–515. https://doi.org/10.1016/J.SOLENER.2021.09.004.

Aste, N., Adhikari, R.S., Del Pero, C., Leonforte, F., 2017. Multi-functional Integrated System for Energy Retrofit of Existing Buildings: A Solution Towards nZEB Standards. Energy Procedia 105, 2811–2817. https://doi.org/10.1016/j.egypro.2017.03.608.

Athienitis, A.K., Barone, G., Buonomano, A., Palombo, A., 2018. Assessing active and passive effects of façade building integrated photovoltaics/thermal systems: Dynamic modelling and simulation. Appl. Energy 209, 355–382. https://doi.org/10.1016/J.APENERGY.2017.09.039.

Attoye, D.E., Aoul, K.A.T., Hassan, A., 2017. A review on building integrated photovoltaic façade customization potentials. Sustainability 9, 2287. https://doi.org/10.3390/su9122287.

Barone, G., Buonomano, A., Forzano, C., Giuzio, G.F., Palombo, A., 2020. Passive and active performance assessment of building integrated hybrid solar photovoltaic/thermal collector prototypes: energy, comfort, and economic analyses. Energy 209, 118435. https://doi.org/10.1016/j.energy.2020.118435.

Barone, G., Buonomano, A., Giuzio, G.F., Palombo, A., 2023a. Towards zero energy infrastructure buildings: optimal design of envelope and cooling system. Energy 279, 128039. https://doi.org/10.1016/J.ENERGY.2023.128039.

Barone, G., Vassiliades, C., Elia, C., Savvides, A., Kalogirou, S., 2023b. Design optimization of a solar system integrated double-skin façade for a clustered housing unit. Renew. Energy 215, 119023. https://doi.org/10.1016/J.RENENE.2023.119023.

Bhamare, D.K., Rathod, M.K., Banerjee, J., 2019. Passive cooling techniques for building and their applicability in different climatic zones—The state of art. Energy Build. 198, 467–490. https://doi.org/10.1016/j.enbuild.2019.06.023.

Buonomano, A., Barone, G., Forzano, C., 2022. Advanced energy technologies, methods, and policies to support the sustainable development of energy, water and environment systems. Energy Rep. 8, 4844–4853. https://doi.org/10.1016/J.EGYR.2022.03.171.

Charalambous, C., Heracleous, C., Michael, A., Efthymiou, V., 2023. Hybrid AC-DC distribution system for building integrated photovoltaics and energy storage solutions for heating-cooling purposes. A case study of a historic building in Cyprus. Renew. Energy 216, 119032. https://doi.org/10.1016/J.RENENE.2023.119032.

Chel, A., Kaushik, G., 2018. Renewable energy technologies for sustainable development of energy efficient building. Alex. Eng. J. 57, 655–669. https://doi.org/10.1016/J.AEJ.2017.02.027.

Conejos, S., Chew, M.Y.L., Tay, K., Tay, S., Safiena, S., 2021. Green maintainability assessment of building-integrated photovoltaic (BIPV) applications: lessons learnt. Int. J. Build. Pathol. Adapt. Ahead–Print. https://doi.org/10.1108/IJBPA-04-2019-0038/FULL/XML.

Čurpek, J., Čekon, M., 2020. Climate response of a BiPV façade system enhanced with latent PCM-based thermal energy storage. Renew. Energy 152, 368–384. https://doi.org/10.1016/J.RENENE.2020.01.070.

Dama, A., Angeli, D., Larsen, O.K., 2017. Naturally ventilated double-skin façade in modeling and experiments. Energy Build. 144, 17–29. https://doi.org/10.1016/J.ENBUILD.2017.03.038.

Energy Performance of Buildings Directive (2018/844/EU), EU, 2018.

F. Escrivà Saneugenio, A. Sateriano, L. Salvati, I. Vardopoulos, Whispers of change: Thirty years for redefining the "Mediterranean City," in: Homage (and Crit. to Mediterr. City. Reg. Sustain. Econ. Resil., River Publishers: Gistrup, Denmark. ISBN: 9788770041775, 2024: pp. 27–64.

Gondal, I.A., Syed Athar, M., Khurram, M., 2021. Role of passive design and alternative energy in building energy optimization. Indoor Built Environ. 30, 278–289. https://doi.org/10.1177/1420326X19887486.

Gustafsson, M., Dipasquale, C., Poppi, S., Bellini, A., Fedrizzi, R., Bales, C., Ochs, F., Sié, M., Holmberg, S., 2017. Economic and environmental analysis of energy renovation packages for European office buildings. Energy Build. 148, 155–165. https://doi.org/10.1016/J.ENBUILD.2017.04.079.

Hasan, A., Alnoman, H., Rashid, Y., 2016. Impact of integrated photovoltaic-phase change material system on building energy efficiency in hot climate. Energy Build. 130, 495–505. https://doi.org/10.1016/j.enbuild.2016.08.059.

Iken, O., Fertahi, S. ed D., Dlimi, M., Agounoun, R., Kadiri, I., Sbai, K., 2019. Thermal and energy performance investigation of a smart double skin facade integrating vanadium dioxide through CFD simulations. Energy Convers. Manag. 195, 650–671. https://doi.org/10.1016/J.ENCONMAN.2019.04.070.

Ioannidis, Z., Buonomano, A., Athienitis, A.K., Stathopoulos, T., 2017. Modeling of double skin façades integrating photovoltaic panels and automated roller shades: Analysis of the thermal and electrical performance. Energy Build. 154, 618–632. https://doi.org/10.1016/j.enbuild.2017.08.046.

Ioannidis, Z., Rounis, E.-D., Athienitis, A., Stathopoulos, T., 2020. Double skin façade integrating semi-transparent photovoltaics: Experimental study on forced convection and heat recovery. Appl. Energy 278, 115647. https://doi.org/10.1016/j.apenergy.2020.115647.

Irshad, K., Habib, K., Algarni, S., Saha, B.B., Jamil, B., 2019. Sizing and life-cycle assessment of building integrated thermoelectric air cooling and photovoltaic wall system. Appl. Therm. Eng. 154, 302–314. https://doi.org/10.1016/J.APPLTHERMALENG.2019.03.027.

Italos, C., Patsias, M., Yiangou, A., Stavrinou, S., Vassiliades, C., 2022. Use of double skin façade with building integrated solar systems for an energy renovation of an existing building in Limassol, Cyprus: Energy performance analysis. Energy Rep. 8, 15144–15161. https://doi.org/10.1016/J.EGYR.2022.11.088.

Kang, D.W., Ryu, J., Konagai, M., 2019. High-Performance Amorphous Silicon Thin Film Solar Cells Prepared at 100 °C: Toward Flexible Building-Integrated Photovoltaics. Electron. Mater. Lett. 15, 623–629. https://doi.org/10.1007/S13391-019-00161-8/FIGURES/5.

Kant, K., Anand, A., Shukla, A., Sharma, A., 2020. Heat transfer study of building integrated photovoltaic (BIPV) with nano-enhanced phase change materials. J. Energy Storage 30, 101563. https://doi.org/10.1016/j.est.2020.101563.

Karytsas, S., Vardopoulos, I., Theodoropoulou, E., 2019. Factors affecting sustainable market acceptance of residential microgeneration technologies. A two time period comparative analysis. Energies 12, 3298. https://doi.org/10.3390/en12173298.

Kundakci Koyunbaba, B., Yilmaz, Z., 2012. The comparison of Trombe wall systems with single glass, double glass and PV panels. Renew. Energy 45, 111–118. https://doi.org/10.1016/J.RENENE.2012.02.026.

Lee, C. sung, Lee, H., Choi, M., Yoon, J., 2019. Design optimization and experimental evaluation of photovoltaic double skin facade. Energy Build. 202, 109314 https://doi.org/10.1016/J.ENBUILD.2019.07.031.

Liu, Z., Zhang, Y., Yuan, X., Liu, Y., Xu, J., Zhang, S., jie He, B., 2021. A comprehensive study of feasibility and applicability of building integrated photovoltaic (BIPV) systems in regions with high solar irradiance. J. Clean. Prod. 307, 127240 https://doi.org/10.1016/J.JCLEPRO.2021.127240.

MATLAB, (1984). mathworks.com.

Michael, A., Savvides, A., Vassiliades, C., Triantafyllidou, E., 2020. Design and Creation of an Energy Efficient Prefabricated Housing Unit based on Specific Taxonomy and Optimization Techniques. Procedia Manuf. 44, 261–268. https://doi.org/10.1016/J.PROMFG.2020.02.230.

Moreno, A., Riverola, A., Chemisana, D., Vaillon, R., Solans, A., 2022. Design and characterization of an OPV-ETFE multi-layer semi-transparent glazing. Energy Rep. 8, 8312–8320. https://doi.org/10.1016/J.EGYR.2022.06.036.

Moreno, Á., Chemisana, D., Lamnatou, C., Maestro, S., 2023. Energy and photosynthetic performance investigation of a semitransparent photovoltaic rooftop greenhouse for building integration. Renew. Energy 215, 118976. https://doi.org/10.1016/J.RENENE.2023.118976.

Ochoa, C.E., Capeluto, I.G., 2008. Strategic decision-making for intelligent buildings: Comparative impact of passive design strategies and active features in a hot climate. Build. Environ. 43, 1829–1839. https://doi.org/10.1016/j.buildenv.2007.10.018.

Papadaki, D., Foteinis, S., Binas, V., N. Assimakopoulos, M., Tsoutsos, T., Kiriakidis, G., Papadaki, D., Foteinis, S., Binas, V., N. Assimakopoulos, M., Tsoutsos, T., Kiriakidis, G., 2019. A life cycle assessment of PCM and VIP in warm Mediterranean climates and their introduction as a strategy to promote energy savings and mitigate carbon emissions, 2019 6944 AIMS Mater. Sci. 6, 944–959. https://doi.org/10.3934/MATERSCI.2019.6.944.

Peng, J., Lu, L., Yang, H., Ma, T., 2015. Comparative study of the thermal and power performances of a semi-transparent photovoltaic façade under different ventilation modes. Appl. Energy 138, 572–583. https://doi.org/10.1016/J.APENERGY.2014.10.003.

Peng, J., Curcija, D.C., Lu, L., Selkowitz, S.E., Yang, H., Zhang, W., 2016b. Numerical investigation of the energy saving potential of a semi-transparent photovoltaic double-skin facade in a cool-summer Mediterranean climate. Appl. Energy 165, 345–356. https://doi.org/10.1016/j.apenergy.2015.12.074.

Peng, J., Curcija, D.C., Lu, L., Selkowitz, S.E., Yang, H., Mitchell, R., 2016a. Developing a method and simulation model for evaluating the overall energy performance of a ventilated semi-transparent photovoltaic double-skin facade. Prog. Photovolt. Res. Appl. 24, 781–799. https://doi.org/10.1002/PIP.2727.

Probst, M.C.M., Roecker, C., 2011. Architectural integration and design of solar thermal systems. EPFL Press.

Rosenow, J., Cowart, R., Bayer, E., Fabbri, M., 2017. Assessing the European Union's energy efficiency policy: Will the winter package deliver on 'Efficiency First'? Energy Res. Soc. Sci. 26, 72–79. https://doi.org/10.1016/J.ERSS.2017.01.022.

Savvides, A., Vassiliades, C., 2017. Designing urban building blocks around solar planning principles. WIT Trans. Ecol. Environ. 226, 679–690. https://doi.org/10.2495/SDP170591.

A. Savvides, C. Vassiliades, I. Vardopoulos, K. Lau, A. Rizzo, A comprehensive exploration of building-integrated photovoltaics and urban design strategies in Luleå, Sweden, and Limassol, Cyprus, Open-Air Cities Institute, Athens, 2024.

Scheinherrová, L., Doleželová, M., Vimmrová, A., Vejmelková, E., Jerman, M., Pommer, V., Černý, R., 2022. Fired clay brick waste as low cost and eco-friendly pozzolana active filler in gypsum-based binders. J. Clean. Prod. 368, 133142 https://doi.org/10.1016/J.JCLEPRO.2022.133142.

B. Schell, J. Esch, SketchUp, (1999). ⟨www.sketchup.com⟩.

Shahrestani, M., Yao, R., Essah, E., Shao, L., Oliveira, A.C., Hepbasli, A., Biyik, E., Caño, T. del, Rico, E., Lechón, J.L., 2017. Experimental and numerical studies to assess the energy performance of naturally ventilated PV façade systems. Sol. Energy 147, 37–51. https://doi.org/10.1016/J.SOLENER.2017.02.034.

Sun, J., Hu, G., Spanos, C.J., 2017. Development and verification of a multizone building HVAC model with TRNSYS. Proc. 2017 12th IEEE Conf. Ind. Electron. Appl. ICIEA 2017 (2018-February), 887–894. https://doi.org/10.1109/ICIEA.2017.8282965.

Theokli, C., Elia, C., Markou, M., Vassiliades, C., 2021. Energy renovation of an existing building in Nicosia Cyprus and investigation of the passive contribution of a BIPV/T double façade system: A case-study. Energy Rep. 7, 8522–8533. https://doi.org/10.1016/j.egyr.2021.03.025.

Tina, G.M., Scavo, F.B., Aneli, S., Gagliano, A., 2021. Assessment of the electrical and thermal performances of building integrated bifacial photovoltaic modules. J. Clean. Prod. 313, 127906 https://doi.org/10.1016/j.jclepro.2021.127906.

Tombazis, A.N., 1994. Architectural design: A multifaceted approach. Renew. Energy 5, 893–899.

TRNSYS, (2019). ⟨http://www.trnsys.com/⟩.

Tsilika, E., Vardopoulos, I., 2022. The FIX-up mix-up; undue façadism or adaptive reuse? Examining the former FIX brewery transformation into the National Museum of Contemporary Art in Athens. Int. J. Archit. Res. Archnet-Ijar. 16, 688–709. https://doi.org/10.1108/ARCH-09-2021-0255/FULL/XML.

Vardopoulos, I., 2018. Multi-criteria decision-making approach for the sustainable autonomous energy generation through renewable sources. Studying Zakynthos Island in Greece. Environ. Manag. Sustain. Dev. 7, 52–84. https://doi.org/10.5296/emsd.v7i1.12110.

Vardopoulos, I., Giannopoulos, K., Papaefthymiou, E., Temponera, E., Chatzithanasis, G., Goussia-Rizou, M., Karymbalis, E., Michalakelis, C., Tsartas, P., Sdrali, D., 2023b. Urban buildings sustainable adaptive reuse into tourism accommodation establishments: a SOAR analysis. Discov. Sustain. 4, 50. https://doi.org/10.1007/s43621-023-00166-2.

Vardopoulos, I., Vannas, I., Xydis, G., Vassiliades, C., 2023a. Homeowners' Perceptions of Renewable Energy and Market Value of Sustainable Buildings, 2023, Vol. 16, Page 4178 Energies 16, 4178. https://doi.org/10.3390/EN16104178.

Vardopoulos, I., Santamouris, M., Zorpas, A.A., Barone, G., Italos, C., Vassiliades, C., 2024a. A Comparative Study on Discrepancies in Residential Building Energy Performance Certification in a Mediterranean Context, 2024, Vol. 14, Page 1009 Build 14, 1009. https://doi.org/10.3390/BUILDINGS14041009.

I. Vardopoulos, F. Escrivà Saneugenio, A. Sateriano, L. Salvati, Homage (and criticism) to the Mediterranean city. Regional sustainability and economic resilience, River Publishers: Gistrup, Denmark. ISBN: 9788770041775, 2024b.

Vassiliades, C., Michael, A., Savvides, A., Kalogirou, S., 2018. Improvement of passive behaviour of existing buildings through the integration of active solar energy systems. Energy 163, 1178–1192. https://doi.org/10.1016/J.ENERGY.2018.08.148.

Vassiliades, C., Kalogirou, S., Michael, A., Savvides, A., 2019. A Roadmap for the Integration of Active Solar Systems into Buildings. Appl. Sci. 9, 2462. https://doi.org/10.3390/app9122462.

Vassiliades, C., Barone, G., Buonomano, A., Forzano, C., Giuzio, G.F., Palombo, A., 2022b. Assessment of an innovative plug and play PV/T system integrated in a prefabricated house unit: Active and passive behaviour and life cycle cost analysis. Renew. Energy 186, 845–863. https://doi.org/10.1016/J.RENENE.2021.12.140.

Vassiliades, C., Agathokleous, R., Barone, G., Forzano, C., Giuzio, G.F., Palombo, A., Buonomano, A., Kalogirou, S., 2022a. Building integration of active solar energy systems: A review of geometrical and architectural characteristics. Renew. Sustain. Energy Rev. 164, 112482 https://doi.org/10.1016/J.RSER.2022.112482.

Vassiliades, C., Minterides, C., Astara, O.E., Barone, G., Vardopoulos, I., 2023. Socio-economic barriers to adopting energy-saving bioclimatic strategies in a Mediterranean sustainable real estate setting: A quantitative analysis of resident perspectives. Energies 16, 7952. https://doi.org/10.3390/en16247952.

Wu, Z., Zhang, L., Su, X., Wu, J., Liu, Z., 2022. Experimental and numerical analysis of naturally ventilated PV-DSF in a humid subtropical climate. Renew. Energy 200, 633–646. https://doi.org/10.1016/J.RENENE.2022.09.108.

Yang, J., Jo, H., Choi, S.W., Kang, D.W., Kwon, J.D., 2018. All p-i-n hydrogenated amorphous silicon oxide thin film solar cells for semi-transparent solar cells. Thin Solid Films 662, 97–102. https://doi.org/10.1016/J.TSF.2018.07.032.

Yesilyurt, M.S., Ozcan, H.G., Yavasoglu, H.A., 2023. Co-simulation-based conventional exergy evaluation of a hybrid energy generation-vanadium redox flow battery-air source heat pump system. Energy 281, 128301. https://doi.org/10.1016/J.ENERGY.2023.128301.